DOI: 10.1002/chem.200800724

# A Novel Platform for Modeling Oxidative Catalysis in Non-Heme Iron Oxygenases with Unprecedented Efficiency

**Anna Company,[a] Laura Gómez,[a] Xavier Fontrodona,[b] Xavi Ribas,[a] and Miquel Costas*[a]**

Non-heme monoiron dependent oxygenases are emerging as a very diverse and versatile group of enzymes involved in a number of oxidative transformations, which also hold potential technological implications.[1] These biological catalysts constitute a source of inspiration for the development of environmentally benign oxidation technologies.[2] On the other hand, bioinspired synthetic catalysts constitute a valuable tool to explore the reaction mechanisms by which non-heme enzymes perform their chemistry.[3] Iron complexes derived from tripodal TPA (TPA = tris(2-methylpyridyl)-amine) and linear BMPEN (BPMEN = *N*,*N*′-bis(2-methylpyridyl)-*N*,*N*′dimethyldiaminoethane) type of ligands are particularly exceptional compounds because of their ability to perform stereoselective enzyme-like transformations such as alkane hydroxylation and alkene epoxidation and *cis*-dihydroxylation, with remarkable efficiency.[3] Such tetradentate backbones wrap around an iron(II) center giving rise to complexes with two *cis* available coordination sites which can be occupied by labile ligands like $CH_3CN$ or $CF_3SO_3$. Parallel to the development of these two families of complexes, several other examples including tri-,[4] tetra-[5] and pentadentate[6] ligands have been explored, yet none of them can compare with TPA and BPMEN families in terms of selectivity, versatility and efficiency.

In this work we report a novel family of non-heme iron complexes based on the methylpyridine derivatized triazacyclononane (TACN) backbone. This novel family of complexes shows unprecedented efficiency in the stereospecific oxidation of alkanes and alkenes with $H_2O_2$, bypassing state-of-the-art oxidations catalyzed by TPA and BPMEN complexes.[3] We show that the type of substitution on the N atoms of the triazamacrocycle and on the pyridine ring are key tools to control the selectivity of the corresponding $Fe^{II}$ complexes in catalytic alkane and alkene oxidation reactions. This structural control of the catalytic selectivity in bioinspired oxidation reactions makes this family of complexes a unique and versatile platform to mimic iron dependent oxygenase-like reactivity.

Reaction of tetradentate ligands $^{R,R'}$PyTACN (Scheme 1) with $Fe(CF_3SO_3)_2(CH_3CN)_2$ in THF afforded title compounds $[Fe(CF_3SO_3)_2(^{R,R'}PyTACN)]$ **1**·$CF_3SO_3$–**4**·$CF_3SO_3$, as white to yellow analytically pure powders that could be obtained in crystalline form after recrystallization from $CH_2Cl_2/Et_2O$.

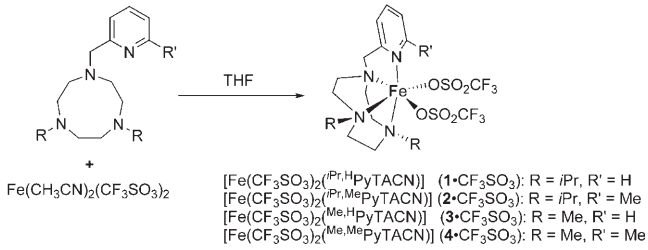


Scheme 1. Complexes described in this work.

Thermal ellipsoid plots corresponding to the X-ray crystallographic characterization of **1**·$CF_3SO_3$ and $[Fe(CH_3CN)_2(^{Me,H}PyTACN)](PF_6)_2$, [**3**·$CH_3CN$]$PF_6$, are shown in Figure 1 to illustrate the structural properties of this family of complexes.[7] The complexes contain iron centers in a distorted octahedral coordination environment. The tripodal tetradentate ligands leave two coordination sites accessible to exogenous ligands ($CF_3SO_3$ or $CH_3CN$) *trans* to non-equivalent aliphatic N atoms (N-$CH_2$-py and $N_{alkyl}$-R, R = $CH_3$ or *i*Pr). The pyridine arm binds *trans* to one of the two $N_{alkyl}$ groups of the ligand. Average Fe–N bond lengths

[a] A. Company, L. Gómez, Dr. X. Ribas, Dr. M. Costas
Departament de Química, Universitat de Girona
Campus de Montilivi, 17071 Girona (Spain)
Fax: (+34) 972-418-150
E-mail: miquel.costas@udg.edu

[b] X. Fontrodona
Serveis Tècnics de Recerca, Universitat de Girona
Campus de Montilivi, 17071 Girona (Spain)

Supporting information for this article is available on the WWW under http://www.chemistry.org or from the author.

 © 2008 Wiley-VCH Verlag GmbH & Co. KGaA, Weinheim 

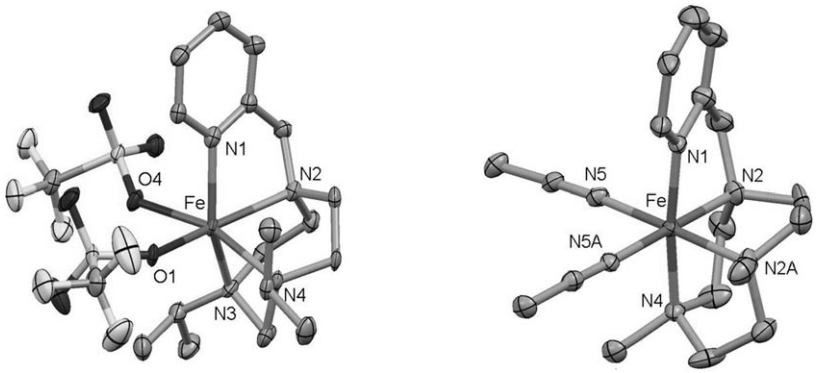


Figure 1. Thermal ellipsoid plot (50% probability) of **1**·$CF_3SO_3$ (left) and [**3**·$CH_3CN$]$PF_6$ (right). Hydrogen atoms have been omitted for clarity.

in **1**·$CF_3SO_3$ and [**3**·$CH_3CN$]$PF_6$ are 2.2 and 2.0 Å, respectively, which are indicative of high and low-spin $Fe^{II}$ configurations.

The catalytic properties of **1**·$CF_3SO_3$–**4**·$CF_3SO_3$ in the hydroxylation of alkanes with $H_2O_2$ are shown in Table 1.[8] Under conditions of large excess of substrate (cyclohexane), **3** and **4** are excellent catalysts and convert up to 76% of $H_2O_2$ into oxidized products, with a remarkably high A/K (alcohol/ketone) ratio. On the other hand, complexes **1** and **2** exhibit significantly lower yields very likely due to the weak tertiary C–H bond of the isopropyl group that renders the complexes susceptible to self-oxidation. The excellent catalytic abilities of **3** and **4** are maintained when larger amounts of peroxide are delivered (see Table 1). When 100 equiv of peroxide are added, catalyst **4** produces 52 TN of alcohol (A) and 12 TN of ketone (K).[9] The efficiency and selectivity exhibited by **4** surpasses those of [Fe($CF_3SO_3$)$_2$(BPMEN)],[3c] the prototypical example of a very active non-heme iron hydroxylation catalyst (48 TN A+K, A/K = 2.5, under identical conditions).

Mechanistic studies, using large excess of substrate to avoid overoxidation reactions, demonstrate the involvement of highly selective metal-centered oxidants. Thus, reactions catalyzed by **3** and **4** exhibit remarkably large A/K ratios (12.3 and 10.2, respectively), and high selectivities as indicated by the kinetic isotope effects evaluated in the oxidation of a 1:3 mixture of cyclohexane/[$D_{12}$]cyclohexane (KIE ≈3–4) and the high $C_{tertiary}/C_{secondary}$ selectivity in the oxidation of adamantane (adam) (3°/2° ≈20–30). In addition, the oxidation of *cis*-1,2-dimethylcyclohexane (DMCH) catalyzed by **3** and **4** exhibits a large degree of stereoretention. However, the same oxidation catalyzed by **1** and **2** shows some degree of loss of stereoretention, which indicates the implication of longer lived carbon centered radicals.

Table 1. Alkane hydroxylation reactions catalyzed by **1**·$CF_3SO_3$–**4**·$CF_3SO_3$.[a]

| Cat | equiv $H_2O_2$ | Cyclohexane $TN_{A+K}$[b] (A/K) | KIE[c] | $H_2O_2/H_2O/O_2$[d] | adam 3°/2°[e] | DMCH RC [%][f] |
|---|---|---|---|---|---|---|
| **1** | 10 | 2.4 (3.6) | 4.8 | 59:8:33 | 14 | 86 |
| **2** | 10 | 0.8 (2.7) | – | 30:3:66 | 21 | 78 |
| **3** | 10 | 6.5 (12.3) | 4.3 | 47:45:8 | 30 | 93 |
| | 100 | 39 (2.6) | – | – | – | – |
| **4** | 10 | 7.6 (10.2) | 3.4 | 85:11:4 | 20 | 94 |
| | 100 | 64 (4.3) | – | – | – | – |

[a] 1000 equiv substrate for cyclohexane and DMCH, 10 equiv for adamantane [b] Turnover number (mols of product/mols of catalyst), A = cyclohexanol, K = cyclohexanone. [c] Kinetic Isotope Effect of cyclohexanol formation. [d] Percentage of oxygen incorporation derived from different sources into the cyclohexanol product. [e] Tertiary/secondary ratio in adamantane (adam) oxidation = 3 × (1-adamantanol)/(2-adamantanol + 2-adamantanone). [f] Percentage of retention of configuration in the oxidation of the tertirary C–H bonds of *cis*-1,2-dimethylcyclohexane (DMCH).

The origin of the oxygen atoms introduced into the cyclohexanol product could be evaluated by means of isotopic labeling experiments performing the oxidation of cyclohexane using 10 equiv $H_2{}^{18}O_2$ in the presence of 1000 equiv $H_2O$ and the complementary experiment using non-labeled $H_2O_2$ and 1000 equiv $H_2{}^{18}O$ (Table 1). It is clearly observed that the incorporation of oxygen atoms from water and/or air into products is highly dependent on the structure of the complexes, suggesting a rich and complex mechanistic scenario modulated by the catalyst architecture. For example, the incorporation of labeled water into cyclohexanol decreases in the order **3** (45%), **4** (11%), **1** (8%) and **2** (3%). On the other hand, incorporation of O derived from air is inversely related to water incorporation; it constitutes more than 30% of the oxidized alcohol product generated by **1** and **2**, but it accounts for less that 10% in the oxidation reactions catalyzed by **3** and **4**. All these evidences indicate that alcohol product is produced via a radical-rebound type mechanism.[3c,10] Competing with this pathway, $O_2$ trapping of the radical followed by Russell-type termination accounts for its incorporation into products. The different level of $O_2$ incorporation into products and DMCH stereoselectivity studies suggest that the lifetimes of the carbon centered radicals are modulated by the particular ligand. On the other hand, the decrease on the A/K ratio when the alcohol concentration increases (compare reactions with 10 and 100 equiv of $H_2O_2$) indicates that the ketone product is most likely formed via oxidation of the initially formed alcohol.[9]

The catalytic ability of **1**–**4** in the oxidation of olefins was also explored and the main results are showed in Table 2. In this case, reactions were run under argon to avoid autooxidation reactions that can occur with olefin substrates. Under large excess of substrate (cyclooctene), all the complexes convert the peroxide into epoxide (E) and diol (D) products, with good to excellent efficiencies expanding from 50 to 81%. Interestingly, the diol/epoxide (D/E) ratio is dramatically modified depending on the catalyst employed.

 © 2008 Wiley-VCH Verlag GmbH & Co. KGaA, Weinheim 

Table 2. Alkene oxidation reactions catalyzed by **1**·$CF_3SO_3$–**4**·$CF_3SO_3$.[a]

| Cat | equiv $H_2O_2$ | Cyclooctene $TN_D$[b] | Cyclooctene $TN_E$[b] | Cyclooctene D/E[c] | Cyclooctene Yield [%][d] | *cis*-2-heptene RC [%][e] epoxide/diol |
|---|---|---|---|---|---|---|
| **1** | 10 | 6.2 | 1.9 | 3.3 | 81 | 88:99 |
| | 100 | 73 | 12 | 6.0 | 85 | – |
| **2** | 10 | 4.5 | 0.5 | 9.0 | 50 | 64:97 |
| | 100 | 10 | 4.0 | 2.5 | 14 | – |
| **3** | 10 | 4.1 | 4.0 | 1.0 | 81 | 93:90 |
| | 100 | 50 | 49 | 1.0 | 99 | – |
| | 300 | 123 | 129 | 0.8 | 77 | |
| **4** | 10 | 6.0 | 1.1 | 5.5 | 71 | 91:90 |
| | 100 | 74 | 12 | 6.2 | 86 | – |
| | 300 | 141 | 29 | 4.9 | 57 | |

[a] 1000 equiv substrate, [b] Turnover number (mol product/mol catalyst), D = *cis*-diol, E = epoxide. [c] D/E = mols of diol/mols of epoxide. [d] Yield based on the oxidant. [e] Percentage of retention of configuration in the oxidation of the C=C bond of *cis*-2-heptene for epoxide and *cis*-diol products.

Thus **3** affords a 1:1 mixture of diol/epoxide and introduction of a methyl group in the pyridine ring (**4**) increases the ratio up to 5.5. Replacement of methyl groups by isopropyl groups in the TACN ring results in better selectivity towards the diol as indicated by the higher selectivity towards *cis*-dihydroxylation exhibited by catalysts **1** and **2**. Interestingly, compound **2** exhibits one of the best selectivities towards *cis*-dihydroxylation among the iron complexes reported in the literature, and it constitutes a functional model of Rieske dioxygenases.[3c,11] The use of larger amounts of peroxide evidences strong differences in the catalytic ability of the complexes. When the peroxide concentration increases 10-fold up to 100 equiv, 73, 50 and 74 TN of *cis*-diol are obtained for **1**, **3** and **4**, respectively. Furthermore, 252 TN (D/E = 0.8) and 170 TN (D/E = 4.9) of products are obtained with **3** and **4**, respectively, when 300 equiv of $H_2O_2$ are used. These numbers are much higher than any previously described iron complex,[3–6,11] and indicate that **1**, **3** and **4** are the most active non-heme iron catalysts for alkene *cis*-dihydroxylation reported so far.[3c,11,12] On the other hand, **2** loses its catalytic activity when the amount of peroxide is increased up to 100 equiv, presumably because of catalyst decomposition. Analogous reactions run under air exhibited smaller D/E ratios mainly because larger amounts of epoxides are obtained (see Supporting Information).

Moreover, oxidation of *cis*-2-heptene indicates that both epoxidation and *cis*-dihydroxylation occur with a large degree of stereoretention, yet significant levels of epimerization suggest that the oxygen atom(s) transfer to the olefin both in epoxidation and in *cis*-dihydroxylation occur in a non-concerted fashion. The higher epoxide yields obtained in reactions run under $O_2$ and the significant levels of epimerization indicate that epoxides are formed in some extent via $O_2$ trapping of carbon centered radical intermediates.[5f]

Labeling studies were performed by running cyclooctene oxidation reactions with 10 equiv $H_2{}^{18}O_2$ in the presence of 1000 equiv $H_2O$, and the complementary experiments were run with 10 equiv $H_2O_2$/1000 equiv $H_2{}^{18}O$ (Figure 2). These

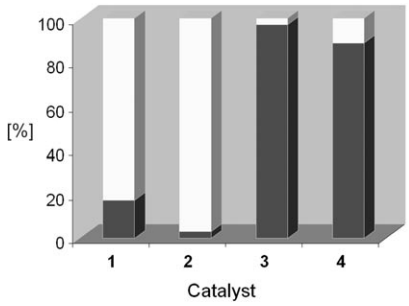


Figure 2. Origin of the oxygen atoms incorporated into the *cis*-diol product in the oxidation of cyclooctene catalyzed by complexes **1**·$CF_3SO_3$–**4**·$CF_3SO_3$. White: percentage of *cis*-diol with the two oxygen atoms originating from $H_2O_2$. Black: percentage of *cis*-diol with one oxygen from $H_2O_2$ and the other from $H_2O$.

experiments indicate a complex mechanistic picture depending on the catalyst. A clear-cut difference arises from *cis*-dihydroxylation reactions catalyzed by **3** and **4** in comparison with **1** and **2**. 90% of the *cis*-diol product obtained in catalytic reactions of **3** and **4** incorporates one O from water and one O from $H_2O_2$, but almost exclusive incorporation of O from $H_2O_2$ is observed for **1** and **2**. Thus, olefin oxidation reactions catalyzed by this family of complexes exhibit a tuned selectivity pattern towards *cis*-dihydroxylation, which resembles that found in TPA and BPMEN families,[3c] yet the present complexes exhibit significantly improved efficiency, and the diol/epoxide selectivity is controlled at two levels: the substitution in the pyridine ring and in the TACN backbone.

Previous studies on related non-heme iron catalysts have shown that isotopic labeling in the *cis*-dihydroxylation reaction is a valuable tool to address the active species responsible for this type of chemistry (Scheme 2).[3,5f]

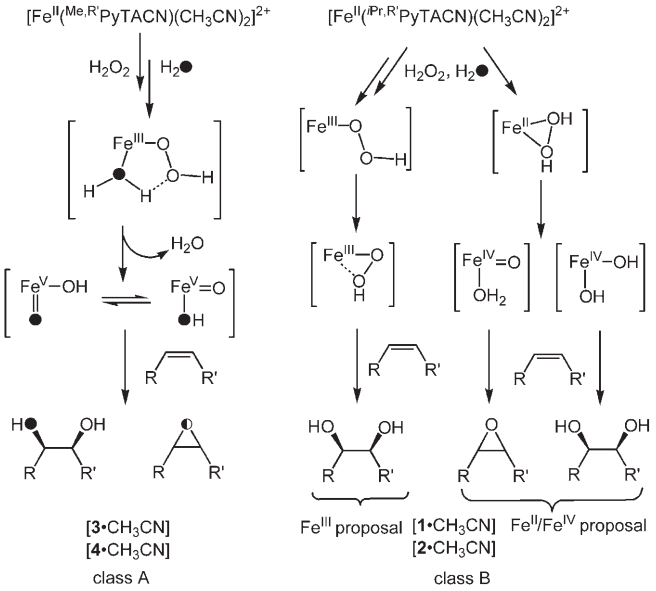


Scheme 2.

 © 2008 Wiley-VCH Verlag GmbH & Co. KGaA, Weinheim 

Class A catalysts insert one atom of oxygen from water and one atom of oxygen from peroxide, and favor epoxidation over *cis*-dihydroxylation, when reacting with olefins. On the other hand, class B catalysts insert both O atoms from peroxide, and favor *cis*-dihydroxylation. The former is an indication of the implication of a $Fe^{V}(O)(OH)$ species via a water assisted O–O lysis,[13] presumably favored by the low-spin state of the iron center, which weakens the hydroperoxide O–O bond (Scheme 2, left).[14] Olefin interaction with the oxo group leads to epoxide, while the *cis*-diol originates from initial attack via the hydroxide ligand.[15] Instead, for class B catalysts two mechanistic scenarios have arisen (Scheme 2, center and right); Que et al. have proposed that a high-spin side-on ferric hydroperoxide or a high valent species, generated with no assistance of water, are the active species responsible for epoxidation and *cis*-dihydroxylation (Scheme 2, center).[3b] On the other hand, Comba et al. have proposed, on the basis of DFT calculations, that O–O bond homolysis of $[LFe^{II}(H_2O_2)]^{2+}$ species (L stands for a tetradentate bispidine ligand) leads to tautomeric species $[LFe^{IV}(OH)_2]^{2+}$ (S=1) and $[LFe^{IV}(O)(OH_2)]^{2+}$ (S=2) (Scheme 2, right).[5f] The former is responsible for the *cis*-dihydroxylation pathway, while the latter accounts for epoxidation activity. Evaluation of these two possibilities for the present systems will require computational analyses which are currently under investigation. In conclusion, isotopic labeling experiments in the *cis*-dihydroxylation reaction led us to conclude that the nature of the alkyl substitution in the TACN ring determines the class dichotomy; catalysts **3** and **4** undergo water assisted O–O lysis and belong to class A, while **1** and **2** belong to class B. Nevertheless, according to this scenario, the significant selectivity for *cis*-dihydroxylation exhibited by **4** is unexpected, and suggests that yet unconsidered factors play a role in the epoxide/diol selectivity. As the exact nature of the reaction mechanism operating in class B catalysts remains a matter of debate, at present it is not clear how does the alkyl substitution in the TACN ring exerts this drastic class selectivity. Nevertheless, the present system constitutes a unique platform that supports both catalytic classes, and thus it is well suited for mechanistic studies on these biologically relevant scenarios.

In conclusion, we have discovered a new family of non-heme iron complexes with unprecedented catalytic activity in bioinspired oxidation reactions. The high selectivity of these reactions along with their degree of stereospecificity suggests the implication of highly selective metal centered species with relevance to the active species involved in non-heme iron enzymes such as naphthalene and toluene oxygenases.[1–2] Recently, White et al. have reported a structurally related complex to the BPMEN system, as stereoselective hydroxylation catalyst for complex organic molecules, albeit with low TN numbers.[16] The excellent catalytic abilities exhibited by **3** and **4** make them a structurally different promising alternative that deserves further exploration. Mechanistic studies and reaction intermediates involved in the reactions, as well as their biological relevance are also currently under investigation.

## Experimental Section

Full experimental details for the preparation of the complexes, details for the crystallographic characterization of **1**·$CF_3SO_3$ and [**3**·$CH_3CN$]$PF_6$ and experimental procedures for catalytic oxidation reactions are included as Supporting Information.

## Acknowledgements

Financial support by MEC-Spain (Project CTQ2006–05367 to M.C.). A.C. and L.G. thank the MEC for FPU-PhD grants. We thank Professor L. Que and Dr. R. Hage for helpful discussions.

**Keywords:** bioinorganic chemistry · enzyme catalysis · model compounds · non-heme oxygenases · oxidation

[1] a) M. Costas, M. P. Mehn, M. P. Jensen, L. Que, Jr., *Chem. Rev.* **2004**, *104*, 939–986; b) M. M. Abu-Omar, A. Loaiza, N. Hontzeas, *Chem. Rev.* **2005**, *105*, 2227–2252.

[2] a) M. Costas, K. Chen, L. Que, Jr., *Coord. Chem. Rev.* **2000**, *200–202*, 517–544; b) S. Tanase, E. Bouwman, *Adv. Inorg. Chem.* **2006**, *58*, 29–75.

[3] a) K. Chen, M. Costas, J. Kim, A. K. Tipton, L. Que, Jr., *J. Am. Chem. Soc.* **2002**, *124*, 3026–3035; b) K. Chen, M. Costas, L. Que, Jr., *J. Chem. Soc. Dalton Trans.* **2002**, 672–679; c) K. Chen, L. Que, Jr., *J. Am. Chem. Soc.* **2001**, *123*, 6327–6337.

[4] a) G. J. P. Britovsek, J. England, S. K. Spitzmesser, A. J. P. White, D. J. Williams, *Dalton Trans.* **2005**, 945–955; b) P. C. A. Bruijnincx, I. L. C. Buurmans, S. Gosiewska, M. A. H. Moelands, M. Lutz, A. L. Spek, G. van Koten, R. J. M. Klein Gebbink, *Chem. Eur. J.* **2008**, *14*, 1228–1237.

[5] a) G. J. P. Britovsek, J. England, A. J. P. White, *Dalton Trans.* **2006**, 1399–1408; b) G. J. P. Britovsek, J. England, A. J. P. White, *Inorg. Chem.* **2005**, *44*, 8125–8134; c) J. England, G. J. P. Britovsek, N. Rabadia, A. J. P. White, *Inorg. Chem.* **2007**, *46*, 3752–3767; d) M. Klopstra, G. Roelfes, R. Hage, R. M. Kellogg, B. L. Feringa, *Eur. J. Inorg. Chem.* **2004**, *4*, 846–856; e) R. Mas-Ballesté, M. Costas, T. van der Berg, L. Que, Jr., *Chem. Eur. J.* **2006**, *12*, 7489–7500; f) J. Bautz, P. Comba, C. Lopez de Laorden, M. Menzel, G. Rajaraman, *Angew. Chem.* **2007**, *119*, 8213–8216, *Angew. Chem. Int. Ed.* **2007**, *46*, 8067–8070; g) M. C. White, A. G. Doyle, E. N. Jacobsen, *J. Am. Chem. Soc.* **2001**, *123*, 7194–7195.

[6] a) S. Gosiewska, M. Lutz, A. L. Spek, R. J. M. Klein Gebbink, *Inorg. Chim. Acta* **2007**, *360*, 405–417; b) S. Taktak, W. Ye, A. M. Herrera, E. V. Rybak-Akimova, *Inorg. Chem.* **2007**, *46*, 2929–2942; c) G. Roelfes, M. Lubben, R. Hage, L. Que, Jr., B. L. Feringa, *Chem. Eur. J.* **2000**, *6*, 2152–2159; d) T. A. van der Berg, J. W. de Boer, W. R. Browne, G. Roelfes, B. L. Feringa, *Chem. Commun.* **2004**, 2550–2551; e) V. Balland, D. Mathieu, N. Pons-Y-Moll, J. F. Bartoli, F. Banse, P. Battioni, J. J. Girerd, D. Mansuy, *J. Mol. Catal. A* **2004**, *215*, 81–87; f) M. R. Bukowski, P. Comba, A. Lienke, C. Limberg, C. Lopez de Laorden, R. Mas-Ballesté, M. Merz, L. Que, Jr., *Angew. Chem.* **2006**, 118, 3524–3528, *Angew. Chem. Int. Ed.* **2006**, *45*, 3446–3449.

[7] Crystal data for **1**·$CF_3SO_3$: $C_{20}H_{32}F_6FeN_4O_6S_2$, monoclinic, $P2_1/c$, $a$=8.994(3) $b$=20.446(6), $c$=15.012(5) Å, $\beta$=91.735(5)°, $V$=2759.4(14) Å$^3$, $Z$=4, $\rho_{calcd}$=1.585 g cm$^{-3}$, $\mu$=0.781 mm$^{-1}$, $T$=100(2) K, crystal size=0.1×0.05×0.01 mm, $\theta$ range=1.99–28.15°, unique reflections=6626, parameters=356, GoF=1.120, R1 [$I>2\sigma(I)$]=0.0650, $w$R2 [$I>2\sigma(I)$]=0.1302. Crystal data for[**3**·$CH_3CN$]$PF_6$: $C_{18}H_{30}F_{12}FeN_6P_2$, monoclinic, $P2_1m$, $a$=7.9099(4), $b$=9.8035(5), $c$=16.6584(9) Å, $\beta$=90.9770(10)°, $V$=1291.58(12) Å$^3$, $Z$=2, $\rho_{calcd}$=1.739 g cm$^{-3}$, $\mu$=0.816 mm$^{-1}$, $T$=100(2) K, crystal size=0.4×0.2×

 © 2008 Wiley-VCH Verlag GmbH & Co. KGaA, Weinheim 

0.1 mm, $\theta$ range = 2.41–28.33°, unique reflections = 3386, parameters = 235, GoF = 1.242, $R1$ [$I > 2\sigma(I)$] = 0.0930, $wR2$ [$I > 2\sigma(I)$] = 0.2102. The asymmetric unit contains half of the molecule. Structure solution and refinement were done using SHELXTL Version 6.14. CCDC 662658 (**1**·$CF_3SO_3$) and CCDC 662659 (**3**·$CF_3SO_3$) contain the supplementary crystallographic data for this paper. These data can be obtained free of charge from The Cambridge Crystallographic Data Centre via www.ccdc.cam.ac.uk/data_request/cif.

[8] Reaction mixtures were analyzed 10 min after $H_2O_2$ addition; longer reaction times did not result in significant differences in reactions efficiencies.

[9] Ketone yield increases with the number of $H_2O_2$ equivalents added (see Table 1) due to overoxidation of alcohol product that also acts as substrate. This was validated by oxidation of cyclohexane in the presence of cyclohexanol (cat **3**/$H_2O_2$/cyclohexane/cyclohexanol 1:100:972:28) that yielded a A/K = 1.75, a value significantly lower than using only 1000 equiv cyclohexane (A/K = 2.6).

[10] A. Company, L. Gómez, M. Güell, J. M. Luis, X. Ribas, L. Que, Jr., M. Costas, *J. Am. Chem. Soc.* **2007**, *129*, 15766–15767.

[11] a) P. D. Oldenburg, A. A. Shteinman, L. Que, Jr., *J. Am. Chem. Soc.* **2005**, *127*, 15672–15673; b) J. Y. Ryu, J. Kim, M. Costas, K. Chen, W. Nam, L. Que, Jr., *Chem. Commun.* **2002**, 1288–1289.

[12] For comparison, oxidation of 1000 equiv cyclooctene with 300 equiv $H_2O_2$ using [$Fe(CF_3SO_3)_2$(BPMEN)] as the catalyst afforded a 47% yield with a D/E ratio of 0.23.

[13] D. Quiñonero, K. Morokuma, D. G. Musaev, R. Mas-Ballesté, L. Que, Jr., *J. Am. Chem. Soc.* **2005**, *127*, 6548–6549.

[14] a) R. Y. N. Ho, G. Roelfes, B. L. Feringa, L. Que, Jr. *J. Am. Chem. Soc.* **1999**, *121*, 264–265; b) N. Lehnert, F. Neese, R. Y. N. Ho, L. Que, Jr., E. I. Solomon, *J. Am. Chem. Soc.* **2002**, *124*, 10810–10822.

[15] A. Bassan, M. R. A. Blomberg, P. E. M. Siegbahn, L. Que, Jr., *Angew. Chem.* **2005**, *117*, 2999–3001; *Angew. Chem. Int. Ed.* **2005**, *44*, 2939–2941.

[16] M. S. Chen, M. C. White, *Science* **2007**, *318*, 783–787.

Received: April 15, 2008
Published online: May 15, 2008

 © 2008 Wiley-VCH Verlag GmbH & Co. KGaA, Weinheim 